JOURNAL OF GEOPHYSICAL RESEARCH, VOL. 112, C07012, doi:10.1029/2006JC003951, 2007

Variable fractal dimension: A major control for floc structure and flocculation kinematics of suspended cohesive sediment

Federico Maggi[1,2]

Received 4 October 2006; revised 15 March 2007; accepted 29 March 2007; published 12 July 2007.

[1] While the fractal dimension of suspended flocs of cohesive sediment is known to vary with the shear rate, electrochemical properties of the sediment and environment, geometrical restructuring, and presence of organic matter, experimental data presented in this work suggest changes in fractal dimension also during floc genesis at constant sedimentological and hydraulic conditions. A power law function is proposed to describe these changes in floc fractal dimension during floc growth and is used to analyze its impact on floc structural parameters, settling velocity, and kinematics of aggregation and breakup. An analysis of this model for the fractal dimension highlights changes of approximately a factor of 2 or more in floc porosity and aggregation and breakup frequencies and of approximately 1 order of magnitude in floc excess density and settling velocity compared to values estimated with constant fractal dimension. The results from this model compare well with prior experimental data collected in situ (Khelifa and Hill, 2006; Manning and Dyer, 1999).

Citation: Maggi, F. (2007), Variable fractal dimension: A major control for floc structure and flocculation kinematics of suspended cohesive sediment, *J. Geophys. Res.*, *112*, C07012, doi:10.1029/2006JC003951.

1. Introduction

[2] Flocculation of suspended cohesive sediment plays a role in the mesoscale and large-scale morphodynamic changes of estuarine environments, coastlines, riverine zones, canals, water basins, etc., through the processes of sediment transport and deposition, which are related to the vertical fluxes of sediment, hence to the floc size and settling velocity distributions. Despite the distributions of size and settling velocity in natural conditions being regulated by many climatological, hydrogeological, biochemical, and physical processes that have an impact on the overall sedimentological behavior of the suspended sediment at manifold time and length scales, one important aspect for the sediment dynamics is represented by the geometrical characteristics of individual flocs. These characteristics, resulting from the small-scale kinematic processes of particle interaction, contribute to determine the shape of the floc size and settling velocity distributions (for example, mode, skewness, etc.), hence the fraction of sediment that is deposited or transported.

[3] Morphological parameters of flocs such as porosity and excess density, as well as the settling velocity, and the kinematic processes of particle aggregation and breakup can be related to their fractal properties. Among many estimators of fractality, for example, the two-dimensional capacity dimension and the perimeter-based fractal dimension, the three-dimensional capacity dimension is the most representative because it describes the space-filling ability of real flocs and can be used in modeling floc morphological parameters, settling velocity, and aggregation and breakup kinematics. The three-dimensional capacity dimension d_3 of floc relates the number of primary particles k to the floc size L as [e.g., *Meakin*, 1998]

$$k = (L/L_p)^{d_3}, \tag{1}$$

with L_p the primary particle size. While d_3 is known to vary with the shear rate [*Stone and Krishnappan*, 2003], electrolyte concentration [*Van Leussen*, 1994; *Berka and Rice*, 2005], presence of microbial biomass [*Van Leussen*, 1994; *Manning and Dyer*, 2002], and with processes of geometrical restructuring from mid to high shear rates [*Thill et al.*, 2001; *Spicer et al.*, 1998; *Oles*, 1992; *Jullien and Meakin*, 1989], a unique value of d_3 is assumed to collectively describe the entire floc population at constant sedimentological and hydraulic conditions, meaning that all flocs have an invariant value of d_3 regardless of their growth stage. Despite this is widely accepted because of the capability to describe self-similar structures resulting from aggregation of fine particles with a constant d_3 [*Meakin*, 1991], statistical self-similarity has experimentally been observed to hold over a floc size range of approximately 1 order only [*Spicer et al.*, 1998; *Johnson et al.*, 1996; *Neimark et al.*, 1996; *Burd and Jackson*, 1997]. It appears therefore questionable whether flocs can be modeled with an invariant scaling within the

[1]Civil and Environmental Engineering, Pratt School of Engineering, Duke University, Durham, North Carolina, USA.
[2]Environmental Fluid Mechanics, Faculty of Civil Engineering and Geosciences, Delft University of Technology, Delft, Netherlands.

0148-0227/07/2006JC003951$09.00

entire size spectrum, which spans about 3 orders of magnitude from the size of the primary particle (micron) to the one of fully developed flocs (millimeter). In addition, as kaolinite minerals and primary particles are crystalline and massive bodies with $d_3 \simeq 3$, while suitably large flocs are porous and irregularly structured bodies with $d_3 < 3$, floc geometry is supposed to experience a transition during growth from Euclidean to fractal.

[4] Data from settling velocity measurements as well as direct observations of floc structure suggest the two- and three-dimensional capacity dimensions decrease as flocculation proceeds in time, i.e., with increasing floc size, also at constant sedimentological and environmental conditions [*Chakraborti et al.*, 2003; *Gardner et al.*, 1998; *Khelifa and Hill*, 2006]. A changing fractal dimension can have a profound consequence on models for floc morphological quantities and on models for flocculation used to determine the floc size and settling velocity distributions. However, the way in which the capacity dimension changes with the floc size during flocculation is not clearly understood and modeled yet, and an analysis of its implications in flocculation models is needed to understand geophysical processes of sediment transport and deposition occurring al large time and length scales.

[5] The aim of this paper is to observe the evolution of kaolinite flocs produced in a turbulent field within a settling column and to assess with imaging techniques how their three-dimensional capacity dimension evolves with the size. These experimental data are used to derive an empirical model for d_3 that is next used to analyze its impact on floc porosity, excess density and settling velocity, and on the kinematics of particle aggregation and breakup.

2. Experiment

2.1. Facility

[6] For the experimental activity, we have used the settling column depicted in Figure 1 with kaolinite mineral of density $\rho_s \approx 2650$ kg/m^3. The minerals size is in the range 0.1–5 μm while stable primary particles have sizes $L_p \approx 5$–20 μm.

[7] A highly concentrated suspension of kaolinite, continuously mixed in the storage tank, is injected into the buffer tank mounted on top of the settling column and is diluted to the test concentration c_d via a controlled system which activates the injection pump when the measured mass concentration in the buffer tank is lower than c_d. Sediment is stirred in the buffer tank with two counter-rotating vanes that produce a recirculating flow and distribute the particles uniformly when entering the settling column, which is 4 m high and 300 mm in diameter. Herein a homogeneous turbulence field, produced by a 4-meter-high oscillating grid consisting of meshes of 75-mm size with square cross-sectioned rods and deck distance of 75 mm, induces flocculation. Flocs pass through the turbulence field and reach the underneath measuring section, where optical recordings are collected with a particle image system consisting of a digital camera that records 8-bit gray scale digital images of 720 × 512 pixel size and a laser diode that illuminates flocs from the side with a light sheet. The camera, focusing a window of about 3 × 2 mm, returns images with 4.16 μm/pixel resolution, where the pixel size ϵ = 4.16 μm approximately corresponds to the smallest primary particle size $L_p \approx 5$ μm. The whole settling column is housed inside a climatized room at $T = 18$°C to minimize temperature gradients and convective flows. The experiment is performed with sediment concentration $c_d = 0.5$ g/l, while the grid is set to oscillate with an amplitude of 84 mm and with frequency calibrated to yield low shear rate $G = 20$ s^{-1}. Finally, the experiment started with no sediment in the column but with a stationary turbulent field.

2.2. Data Collection and Treatment

[8] Flocs are recorded on digital tapes in a series of movies, each of the duration of 7 minutes, repeated every 3 hours for 7 days. Individual frames are extracted from each movie in a way such to not count more than once the same flocs in the camera view and to have statistically representative floc populations within each movie. In this way, a sequence of floc size distributions is produced at times $t = \{0,3, 6,\ldots\}$ hours and used to study changes of the fractal dimension of flocs in time.

[9] Frames selected from these movies are converted into black-and-white with the procedure already used in the work of *Maggi et al.* [2006]. From these, the size L of every floc is computed as the length of the smallest square embedding the floc shape, while the two-dimensional perimeter-based fractal dimensions

$$d_P = 2 \cdot \log(P)/\log(A),$$

is calculated from the dimensionless floc perimeter P and area A, with $1 \leq d_P \leq 2$. The three-dimensional capacity dimension d_3^* of individual flocs is assessed from d_p as [*Maggi and Winterwerp*, 2004]

$$d_3^* = \left(\frac{a(\ell)}{d_P - b(\ell)}\right)^{1/2}, \tag{2}$$

where $\ell = L/\epsilon \approx L/L_p$ is the dimensionless floc size, with the primary particle size $L_p \approx \epsilon$. The functions $a(\ell)$ and $b(\ell)$ are used to take into account the resolution at the detector and are known for any ℓ

$$a(\ell) = 9[z(\ell) - b(\ell)], \quad b(\ell) = \frac{2[k(\ell)]^2 - 9z(\ell)}{[k(\ell)]^2 - 9},$$

with $k(\ell) = z(\ell)[z(\ell) - 1] + 1$ and $z(\ell) = \log[4\ell - 4]/\log[\ell]$. Equation 2 is valid in the full range $1 \leq d_P < 2$, i.e., except for projections having $A \equiv P$, and can return values of d_3 in the range $1 \leq d_3 < 3$. Because of this, equation 2 can circumvent the rule [*Falconer*, 1990]

$$d_3^* \begin{cases} = d_2 & \text{for } d_2 < 2, \\ \geq 2 & \text{for } d_2 = 2, \end{cases} \tag{3}$$

which is limited to projections whose two-dimensional capacity dimension is $d_2 < 2$, hence to values of d_3 in the range $1 \leq d_3 < 2$. Equation 2 was tested in the work of *Maggi* [2005] in reconstructing the three-dimensional capacity dimension of random fractal aggregates obtained by diffusion-limited aggregation (DLA) and cluster-cluster aggregation (CCA) processes from their two-dimensional projections and was shown to return values of d_3 with mean

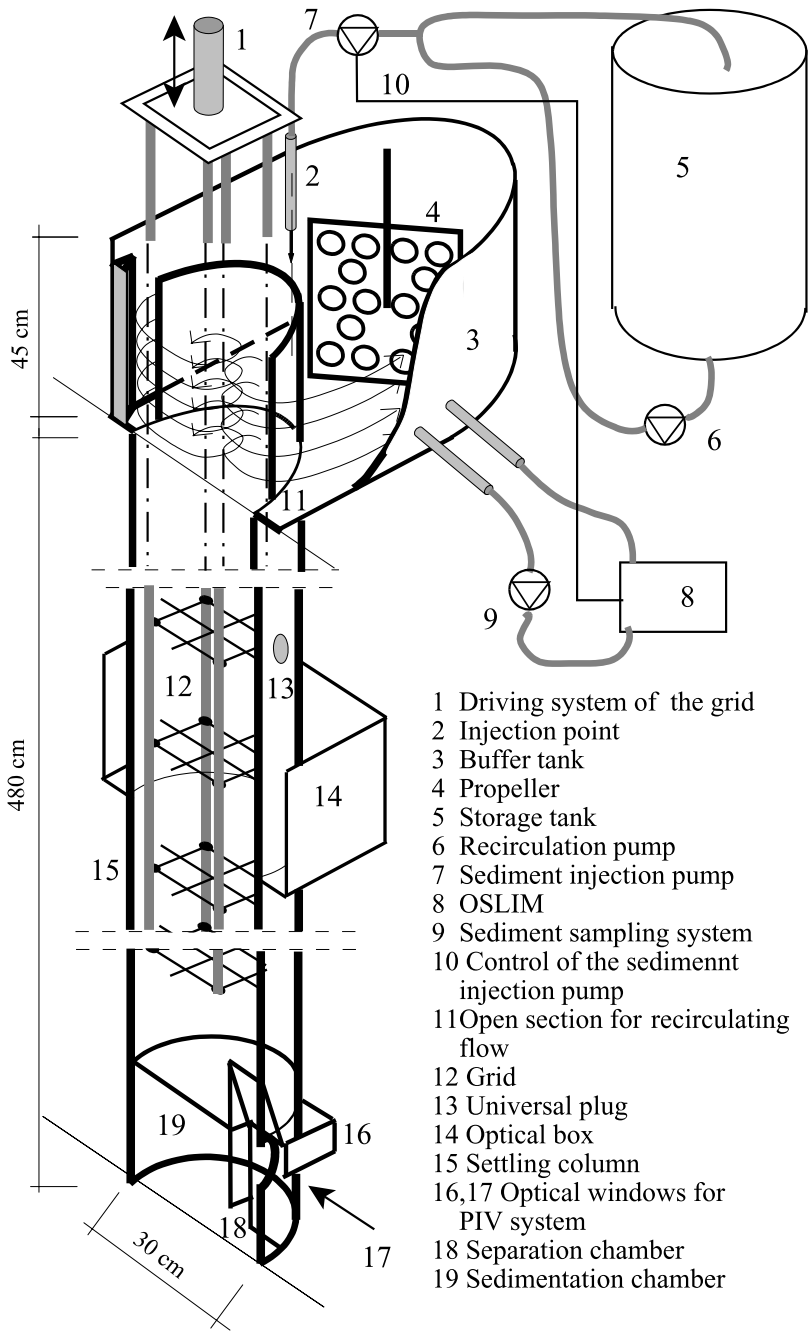

Figure 1. Schematic view of the longitudinal cross section of the settling column used in our experimental campaign. Functioning and characteristics are described in detail in the work of *Maggi et al.* [2002].

squares errors $E = 0.004$ compared with $E = 0.018$ and $E = 0.054$, respectively, obtained using equation (3).

2.3. Experimental Results

[10] The three-dimensional capacity dimension is analyzed for flocs in nonequilibrium and in steady state populations. While the nonequilibrium populations are represented by flocs observed shortly after the initial sediment injection in the column, the time beyond which the population can be considered at steady state is determined experimentally from the variations of the floc size distributions between two sequential recordings and from the flocculation timescale T_f in the settling column, estimated to be $T_f \approx 25$ hours. We focus our analysis on four data sets recorded at times $t = \{0, 3\}$ hours (i.e., nonequilibrium floc populations) and at times $t = \{162,165\}$ (i.e., steady state floc populations), respectively, whose floc size distributions are depicted in Figure 2a.

[11] The values of d_3^* computed with equation (2), represented in the double-logarithmic plot of Figure 2b, decrease with increasing dimensionless size ℓ, meaning that flocs appear increasingly clustered or filamentous as L increases. Figure 2b suggests d_3 to follow a power law of L

$$d_3(L) = \delta \ell^{\xi} = \delta \left(L/L_p\right)^{\xi}, \tag{4}$$

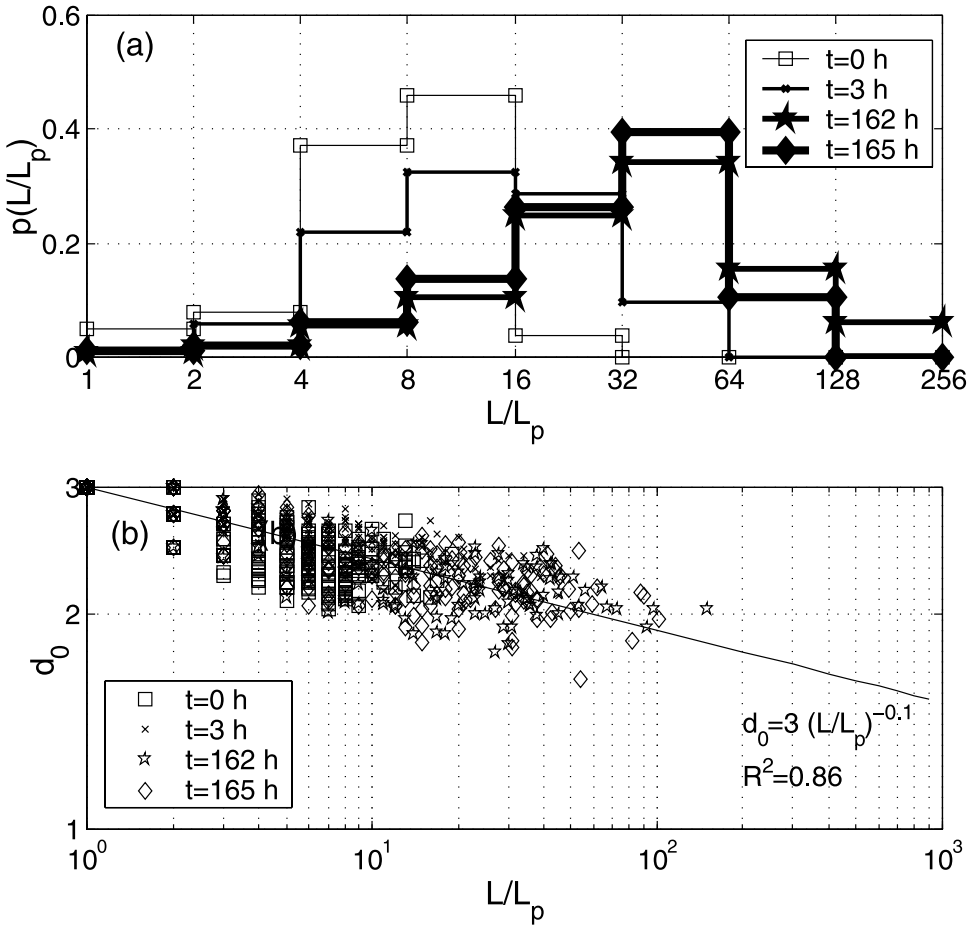

Figure 2. (a) Floc size distribution measured in the settling column of Figure 1 at times $t = \{0, 3, 162, 165\}$ hours. (b) Relationship between the dimensionless size $\ell = L / L_p$ and the three-dimensional capacity dimension d_3 of the flocs at the same experimental times of data in Figure 2a (redrawn from the work of *Maggi* [2005]).

where δ and ξ are estimated by data fitting (Table 1). The parameter δ can be interpreted as the capacity dimension of the primary particles, and it can be taken $\delta = 3$ (Table 1). This value harmonizes with the fact that primary particles have size $L = L_p \approx \epsilon$ and are stacks of massive, Euclidean crystals with $d_3 = 3$. Therefore a pixel size $\epsilon \approx L_p$ does not compromise the information of fractality of the primary particles at the detector and optimizes the use of the optics for larger flocs. The parameter ξ, instead, represents the rate at which d_3 decreases for $L > L_p$ and, as suggested by Table 1, can be taken $\xi = -0.1$. These values of δ and ξ are valid for flocculated kaolinite minerals and correlate to experimental data with an $R^2 = 0.859$. Nevertheless, equation (4) allows to use other values of ξ to describe better the decay in d_3 for suspensions of different nature, as well as $\xi = 0$ and $\delta < 3$ when all flocs and primary particles are characterized by an identical capacity dimension $d_3 = \delta < 3$.

[12] It is note worthy that δ and ξ are substantially invariant in time, that is, they do not change during the phase transition of the floc population from nonequilibrium to steady state.

[13] Equation (4) is limited to the range of L/L_p for which $1 \leq d_3 \leq 3$, where the upper boundary is obvious for physical reasons, and the lower boundary is due to the fact that flocs with $d_3 < 1$ would be two disjoint masses rather than a unique floc. In the upper boundary, onset of flocculation is characterized by flocs that experience a structural crossover from Euclidean to fractal occurring as soon as ℓ becomes $\ell > 1$. The Euclidean-to-fractal crossover at this initial stage of growth may be characterized by a discontinuity not taken into account by equation (4). Consider k primary particles having $d_3 = \delta = 3$ to attach to each other forming a line-like chain with dimensionless linear size $\ell = L/L_p = k$; the capacity dimension of this newly formed floc will be $d_3 = \log[k]/\log[k] = 1$, which is smaller than $d_3 = 3k^{-0.1}$ for small k. However, the probability that all k primary particles collide to form such structure is very low for aggregates forming in turbulent fields. In addition, this

Table 1. Values of δ and ξ Resulting From Least Square Fitting to the Data at Times $t = \{0, 3, 162, 165\}$ Hours[a]

Time t State	0 NE	3 NE	162 SS	165 SS
δ	3.437	3.378	3.357	3.359
ξ	−0.112	−0.079	−0.093	−0.092
R^2	0.847	0.830	0.863	0.859

[a]NE and SS refer to non-equilibrium and steady state, respectively.

"jump" should be evident only for $k = 2$ and should vanish quickly during the initial exponential growth phase, when the number of primary particles in a floc increases rapidly. Similarly, if we consider monosized primary particles with $L_p = 5$ μm, the size L^* corresponding to the lower boundary ($d_3 = 1$) is $L^* = L_p\,(1/\delta)^{1/\xi} = 5 \times 5.9 \times 10^{-2}$ m ≈ 30 cm. This is hardly reached by real sediment flocs in natural conditions. Thereby, equation (4) can describe decreases in d_3 over a broad range of floc sizes in real conditions.

[14] Furthermore, it is generally observed for the modal floc size to scale with the shear rate as $\widetilde{L} \propto G^x$ with $x < 0$ [e.g., *Lick et al.*, 1993], meaning that increases in G produce smaller flocs. If we substitute this scaling into the power scaling $d_3 \propto \widetilde{L}^{\xi}$ of equation (4) where $\xi < 0$, we obtain the new scaling $d_3 \propto G^{x\xi}$ with $x\xi > 0$. This predicts an average increase in capacity dimension for flocs subject to increases in G, the behavior which has been observed in the work of *Stone and Krishnappan* [2003].

[15] While the physical process responsible for the formation of fractal structure from Euclidean particles can be related to shielding effects [*Ball and Blunt*, 1989], which is internal throats of flocs are less accessible to particles than the surface, the decrease in capacity dimension with increasing floc size can be related to a gradual transition from Brownian flocculation at initial states (i.e., when small particles collide and attach prevalently because of Brownian diffusivity), toward cluster-cluster flocculation (i.e., when larger flocs collide and attach mainly because of shear flow and differential settling) [*Farley and Morel*, 1986; *Burd and Jackson*, 1997]. These two regimes can be associated to DLA and CCA processes, respectively, which result in the formation of randomly structured fractal flocs well-known to be characterized by three-dimensional capacity dimensions $d_3 \approx 2.5$ for DLA and $d_3 \approx 1.8$ for CCA [*Vicsek*, 1992].

[16] A model for variable capacity dimension carries an advantage in describing floc geometry and mass-density distribution within the fractal theory. A detailed description of this is beyond the purpose of this paper, but the main directions are introduced in the following.

[17] While the capacity dimension is a measure of the portion of a space of characteristic length L occupied by a body, a rich description of how mass is distributed within this space can be achieved by means of the generalized dimensionality, which is represented through the multifractal spectrum f [*Hentschel and Procaccia*, 1983; *Grassberger and Procaccia*, 1983; *Chhabra and Jensen*, 1989; *Meakin*, 1998]. The infinite number of fractal dimensions in f describe the distribution of mass in nonhomogeneous compact (close and finite) bodies over the infinite number of length scales comprised within the cut offs [*Argyris et al.*, 1994]. Multifractal analysis, successfully used to study the monoscale and multiscale nature of DLA and CCA aggregates [*Meakin*, 1998], was performed on floc shapes collected in the settling column showing that growing flocs are marked by a progressively widening spectrum f, and by $\sup\{f\}$ decreasing as the floc size increases [*Maggi*, 2005], where $\sup\{f\}$ corresponds to the capacity dimension [*Grassberger and Procaccia*, 1983]. The use of $d_3 = \text{const} < 3$ for all flocs, therefore, does not add any specific information of the floc mass-density distribution, i.e., of their monoscale or multiscale (multifractal) geometry. Conversely, a decreasing d_3 implies an evolution of the mass-density distribution from monoscale to multiscale that can be associated to, and modeled with, a widening spectrum f. This will be part of a future mathematical analysis of the evolution of floc geometry, while in the present study we focus on the impact of a changing d_3 on hydraulic and geometric floc quantities.

3. Structural and Hydraulic Parameters of Flocs for Variable Fractal Dimension

[18] The impact of a changing capacity dimension d_3 on structural parameters and settling velocity of flocs is explored for various values of the primary particle capacity dimension δ and exponent ξ of the power law in equation (4).

[19] Upon substitution of equation (4) into equation (1) we obtain the scaling law

$$k = (L/L_p)^{d_3(L)} = (L/L_p)^{\delta(L/L_p)^{\xi}}, \tag{5}$$

which allows to determine the size L of a floc given k, L_p, ξ, and δ. Figure 3a shows that increases in ξ determine a more rapid increase in L for increasing primary particle number k, whereas decrease in ξ, vice versa, determine a less rapid increase in L. The effect of a decreasing capacity dimension δ of the primary particles always determines more rapid increases in L than with $\delta = 3$ (Figure 3b), hence with an overall effect similar to decreases in ξ. For this reason, we limit the following analyzes to variations in the rate of change ξ.

[20] Consider a massive floc of size L with $d_3 = 3$ and made of $n = (L/L_p)^3$ primary particles; consider also a fractal floc of the same size but with $d_3(L) < 3$ made of $k = (L/L_p)^{d3(L)} < n$ primary particles. The porosity e, given by the ratio $e = (n - k)/n$ with $(n - k)$ the dimensionless measure of voids, can be written in terms of capacity dimension

$$e = 1 - (L/L_p)^{d_3(L)-3}, \tag{6}$$

and can be used to determine the floc excess (effective) density $\Delta\rho_e$ [*Kranenburg*, 1994; *Sterling et al.*, 2005]

$$\Delta\rho_e = \rho_f - \rho_w = (\rho_s - \rho_w)\left(\frac{L_p}{L}\right)^{3-d_3(L)} = (\rho_s - \rho_w)(1 - e), \tag{7}$$

with ρ_f, $\rho_s = 2500$ kg/m^3, and $\rho_w = 1000$ kg/m^3 the floc, sediment and water densities, respectively. If we take $d_3 = \text{const} = 2$ as the reference value averagely used in modeling fractal flocs [e.g., *Flesch et al.*, 1999; *Zhang and Li*, 2003; *Kunster et al.*, 1997], the effect of a changing d_3 on e is especially evident on flocs with $L < 100$ μm, which show a lower porosity compared to those with $d_3 = 2$ (Figure 4a). This is in agreement with the fact that e increases with L for fractal flocs and has the advantage to circumvent single or multiple discontinuities introduced by "core-shell" models that conceptualize flocs as massively packed in the center and open near surface [*Kunster et al.*, 1997; *Wu et al.*, 2002; *Veerapaneni and Wiesner*, 1996; *Li and Logan*, 2001]. Decreasing values of ξ tend to produce more porous flocs

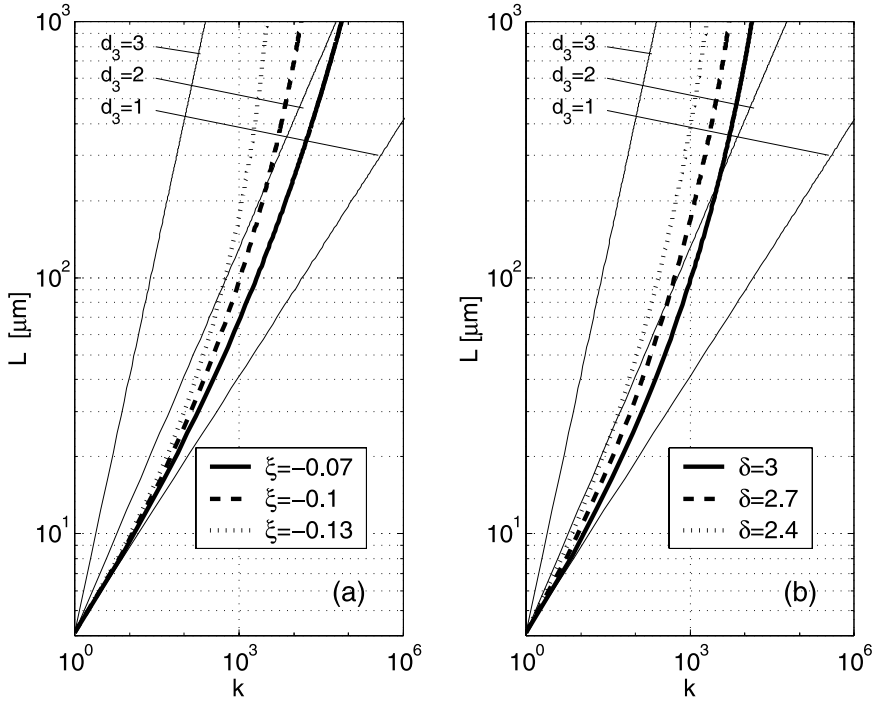

Figure 3. Analytical relationship between primary-particle number k and floc size L for various values of the (a) exponent ξ of equation (4) and (b) primary particle capacity dimension δ.

(Figure 4a). Decreases in δ have a similar effect on e (data not shown).

[21] Analogously, a variable $d_3(L)$ has the effect of causing a more gentle decrease in effective density $\Delta\rho_e$ at small floc sizes ($L < 30$ μm) with respect to the one computed with $d_3 = 2$, and a more rapid decrease for $L > 30$ μm (Figure 4b). Decreases in ξ accentuate further this behavior. These modeling data resemble with good agree-

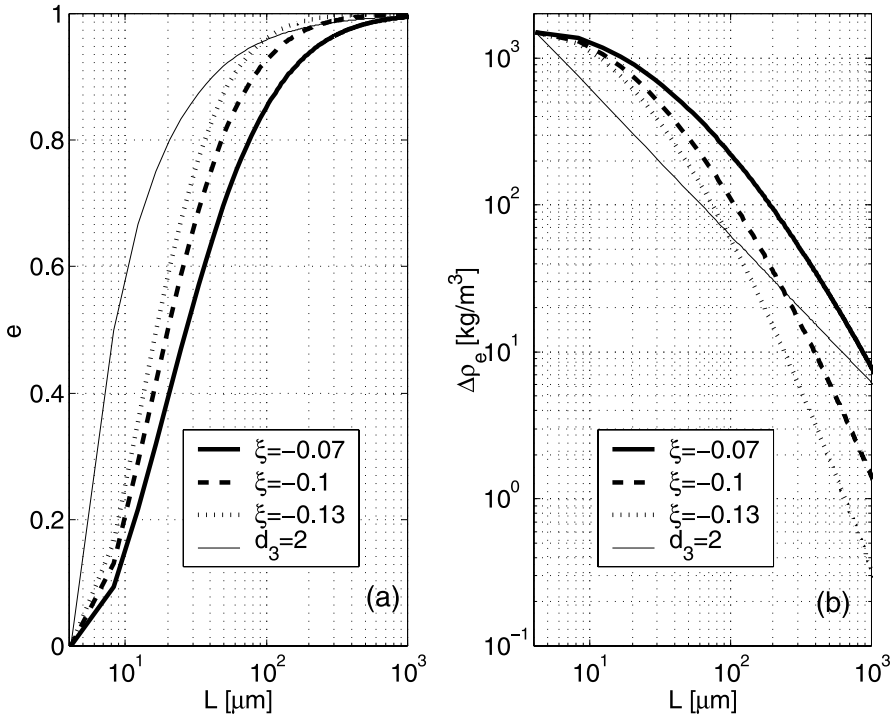

Figure 4. (a) Relationship of porosity e and (b) excess density $\Delta\rho_e$ as functions of L for constant and variable capacity dimensions d_3. In both panels d_3 = const = 2, while variable capacity dimension is computed with $\delta = 3$ and various values of ξ. Differences from using equation (4) and $d_3 = 2$ can be of a factor of 2 in e and of 1 order of magnitude in $\Delta\rho_e$.

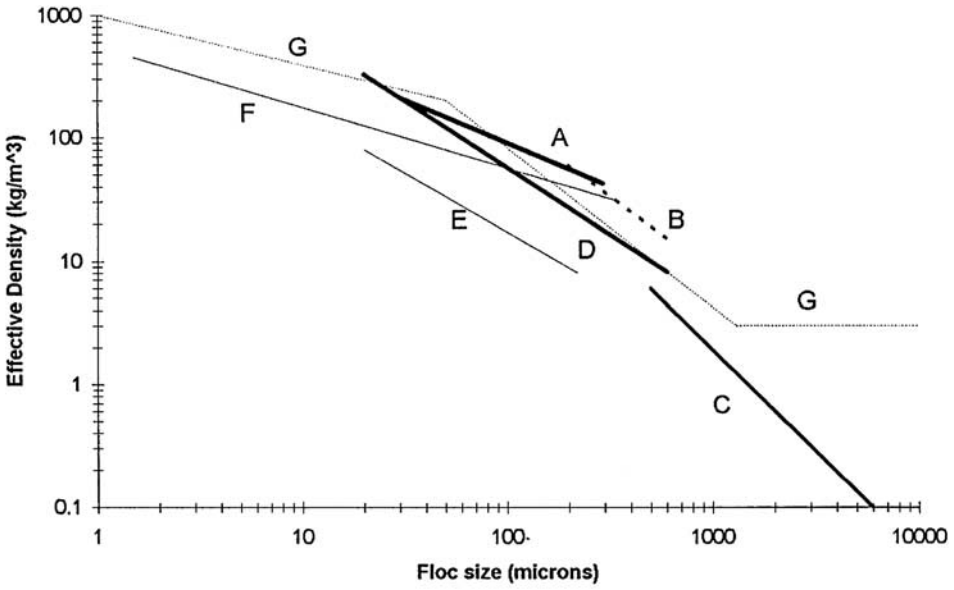

Figure 5. Experimental effective density $\Delta\rho_e$ for several sediment floc samples (labeled as A through G) redrawn from the work of *Manning and Dyer* [1999]. This plot shows an overall trend well reproduced by the model for variable fractal dimension of equation (4) represented in Figure 4b.

ment several experimental data sets grouped together and analyzed on a wider floc size range in the work of *Manning and Dyer* [1999] showing that $\Delta\rho_e$ becomes gradually more sloped for increasing floc size (Figure 5).

[22] By substituting equation (7) into the Stokes' law for the settling velocity of spherical nonporous particles with a Reynolds number smaller than 1, mathematically written as

$$v = \frac{(\rho_f - \rho_w)g}{18\mu} L^2, \tag{8}$$

we obtain an expression for the settling velocity of fractal flocs

$$v = (1-e)\frac{(\rho_s - \rho_w)g}{18\mu} L^2 = \frac{(\rho_s - \rho_w)g}{18\mu} \frac{L_p^{3-d_3(L)}}{L^{1-d_3(L)}} \tag{9}$$

[23] Data in Figure 6a show that a capacity dimension decreasing with L can have a profound impact on the floc velocity, which increases with L up to a maximum at a floc size L^*, beyond which, it decreases. This behavior of the settling velocity can be explained in terms of porosity; in fact, an increasing porosity $e \rightarrow 1$ (Figure 4) has the effect to decrease $\Delta\rho_e \rightarrow 0$, hence to decrease also $v \rightarrow 0$ as formulated via equation (9). A decreasing ξ causes L^* to move toward smaller sizes, thus resulting in a further reduction of the falling velocity of large flocs compared to midsized flocs. For primary particles with capacity dimension δ progressively smaller than 3, the settling velocity becomes accordingly smaller, with L^* less sensitive to variations in δ than to variations in ξ (Figure 6b).

[24] Single experimental observations that can characterize in a general manner the behavior of the settling velocity over a wide range of floc sizes are scarce. However, a long history in measuring the floc settling velocity in natural waters has resulted in an ample database detailedly compiled in the work of *Khelifa and Hill* [2006]. In their work, Khelifa and Hill have grouped together data from 20 published works giving an important picture of the settling velocity over approximately 4 orders of magnitude in floc size. Figure 7, taken from the work of *Khelifa and Hill* [2006], shows that the curved behavior anticipated by equation (9) for the settling velocity with increasing L finds good agreement with experimental data.

[25] We do not rule out that different expressions to account for variations in capacity dimension can equally explain the behavior in excess density and settling velocity discussed above. Yet, Figure 2b gives an underpinning clue that this must depend on structural and geometric properties of the flocs. Nonetheless, it is of surprising interest to note that while our power law model of the three-dimensional capacity dimension was derived from direct optical observation of the floc structure, *Khelifa and Hill* [2006] have derived a power law function similar to equation (4) from the data of Figure 7. It appears therefore meaningful to consider the capacity dimension a variable quantity, which changes as a power law function during floc growth, also at constant sedimentological and environmental conditions.

4. Aggregation and Breakup Kinematics for Variable Fractal Dimension

[26] The analyses of section 3 show that a variable capacity dimension $d_3(L)$ largely impacts the structural parameters and the settling velocity of flocs. As these play a direct role in particle-particle interactions [e.g., *Berka and Rice*, 2005; *Sato et al.*, 2004; *Li and Logan*, 2001; *Winterwerp*, 1998; *Kunster et al.*, 1997; *Veerapaneni and Wiesner*, 1996], a variable capacity dimension can in turn impact the aggregation and breakup rates with an

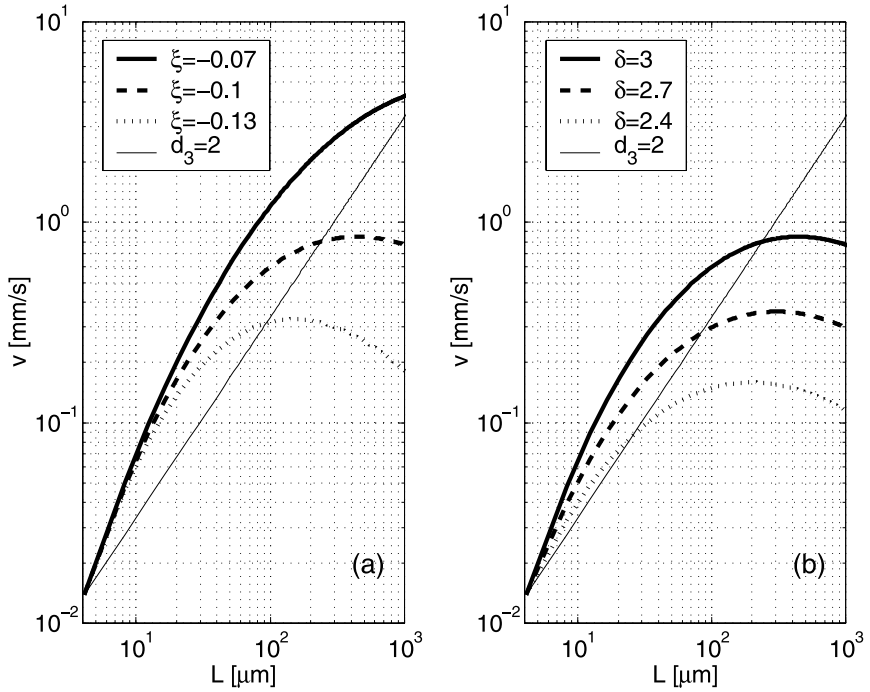

Figure 6. Relationship between floc size L and settling velocity v for constant and variable capacity dimensions d_3 computed for various values of (a) ξ and (b) δ. Difference from using equation (4) and $d_3 = 2$ can be nearly of 1 order of magnitude for $\delta = 3$ or more for $\delta < 3$.

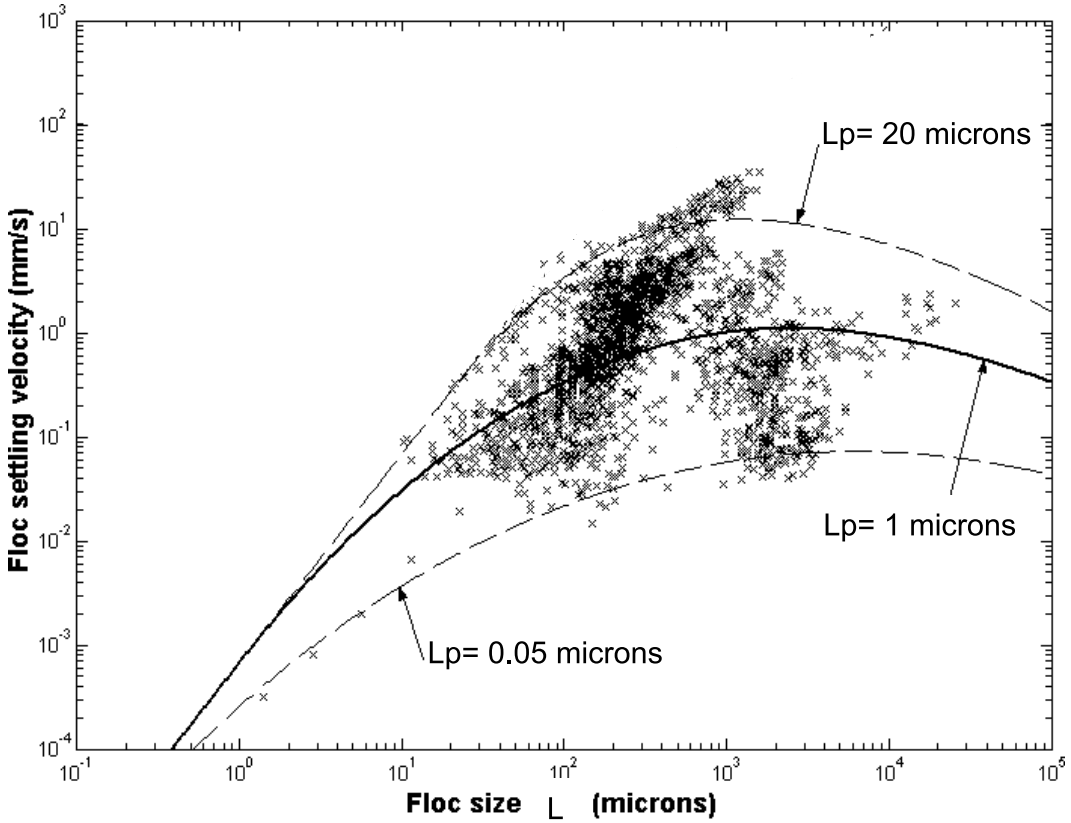

Figure 7. Experimental floc settling velocity as a function of floc size from the work of *Khelifa and Hill* [2006]. Solid and dashed lines represent best and boundary fitting from Khelifa and Hill's model. These experimental data are replicated well by the settling velocity model with variable capacity dimension in Figure 6.

important effect on the time evolution of the floc size distribution. The equilibrium floc size and settling velocity distributions, moreover, depend not only on the velocity of the aggregation and breakup reactions but also on the balance between the two. The way in which the scaling relationship between floc mass and size changes during floc growth, and the rate at which the reactions of aggregation and breakup change with the floc size and capacity dimension, depends on the exponent ξ and the parameter δ of equation (4). The following analysis is therefore aimed at indicatively showing the impact of porous flocs modeled with variable fractal dimension on the aggregation and breakup rates.

[27] In the population balance equations used to model flocculation of cohesive sediment [e.g., *Burban et al.*, 1989; *Lick et al.*, 1993; *Flesch et al.*, 1999; *Zhang and Li*, 2003; *Kunster et al.*, 1997], the rate of particle aggregation is normally modeled as the product $\alpha\Lambda_{i,j}$, with $\Lambda_{i,j}$ expressing the frequency of collision between two particles and α expressing the likelihood of these to attach after collision.

[28] The collision frequency $\Lambda_{i,j}$ can be expressed as $\Lambda_{i,j} = \Lambda_{i,j}^{\mathrm{BM}} + \Lambda_{i,j}^{\mathrm{DS}} + \Lambda_{i,j}^{\mathrm{TS}}$ because of the contributions of Brownian motion (BM), differential settling (DS), and turbulent shear (TS), respectively [e.g., *Hunt*, 1980; *Serra and Casamitjana*, 1998a, 1998b]

$$\Lambda_{i,j}^{\mathrm{BM}} = \frac{2KT(L_i + L_j)^2}{3\mu L_i L_j}, \tag{10}$$

$$\Lambda_{i,j}^{\mathrm{TS}} = \frac{G}{6}(L_i + L_j)^3, \tag{11}$$

$$\Lambda_{i,j}^{\mathrm{DS}} = \frac{\pi}{4}(L_i + L_j)^2 |v_i - v_j|. \tag{12}$$

[29] Despite not accounting for the Van der Waals and electrostatic potentials resulting in the "double-layer barrier" (zeta potential), equations (11) and (12) have widely been used in mechanistic models of flocculation in virtue of the fact that, in aqueous media, the shear rate G and the settling velocity v can become more important than electrochemical potentials in particle collision. It is note worthy that, instead, equations (10), (11), and (12) do not take into account hydrodynamic interactions, which can become important for same ranges of G, L, and e. For instance, the collision frequency has experimentally been observed to decrease for $|L_i - L_j|$ increasing because of hydrodynamic shielding [*Stolzenbach and Elimelech*, 1993]. An increasing porosity, instead, has been reported to diminish the hydrodynamic shielding because of the flow through the porous structure of two approaching flocs [*Li and Logan*, 1997; *Kim and Yuan*, 2005]. Other more complicated (for example, curvilinear) models can be used to estimate the collision frequencies taking into account electrochemical potentials but require a larger number of parameters and still lack in description of the hydrodynamic interaction of porous fractal flocs [e.g., *Li and Logan*, 1997].

[30] The collision efficiency α, instead, is generally assumed to be either $\alpha = 1$ [e.g., *Farley and Morel*, 1986; *Krishnappan*, 1990] or a calibration parameter for which any collision between any two differently sized flocs will occur with the same likelihood of success [e.g., *Serra and Casamitjana*, 1998c; *Lick and Lick*, 1988]. Recently, also the collision efficiency between porous flocs was observed to not be constant for differently sized particles [*Sterling et al.*, 2005] and to increase with floc porosity [*Kim and Stolzenbach*, 2004].

[31] In the following, we aim at writing an aggregation rate $\alpha_{i,j}\Lambda_{i,j}$ that takes into account hydrodynamic effects due to the size and porosity of flocs in a relatively simple mathematical manner. Earlier works [e.g., *Friedlander*, 1957, 1965; *McCave*, 1984] have proposed formulations of α as functions of L, but none led to a generalizable exact solution. Arbitrarily, we examine the collision efficiency proposed by *Pruppacher and Klett* [1978], $\alpha_{i,j} = (L_i/L_j)^2/(2(1 + L_i/L_j)^2)$ with $L_i \leq L_j$, as this is simpler than and essentially equivalent to the others in terms of overall behavior. This formulation of α can be extended to include hydrodynamic effects due to floc porosity via a factor written as a function of the capacity dimension of the flocs. In particular, a modified Pruppacher and Klett's collision efficiency can be written as

$$\alpha_{i,j} = \frac{9}{d_3(L_i)d_3(L_j)} \frac{(L_i/L_j)^2}{2(1 + L_i/L_j)^2}, \text{ with } L_i \leq L_j. \tag{13}$$

By using equations (10), (11), (12), and (13) to calculate the effective aggregation rate $\alpha_{i,j}\,\Lambda_{i,j}$, we introduce in a simple and compact form the hydrodynamics effects of floc size and porosity during aggregation.

[32] An inspection of $\alpha_{i,j}$, Figure 8, shows that for $L_j \gg L_i$, $\alpha_{i,j}$ tends to decrease because of the ratio $L_i/L_j \ll 1$ and to increase because of a $d_3(L_j) < d_3(L_i) < 3$. Moreover, $\alpha_{i,j}$ tends to generally increase when both flocs are large. Equation (13) reproduces in a qualitative way the behavior described in the works of *Kim and Yuan* [2005], *Kim and Stolzenbach* [2004], *Sterling et al.* [2005], and *Stolzenbach and Elimelech* [1993] and can be used as a first indication for assessing the effective aggregation frequency. In addition, by using equation (4), a decreasing ξ increases the overall sticking probability for both small and large colliding flocs. A decreasing primary particle capacity dimension δ affects $\alpha_{i,j}$ in a way similar to a decreasing ξ (data not shown).

[33] Finally, the rate B at which flocs break up has been related to L, L_{p}, G, floc strength, and other quantities via various scaling relationships. Yet, none of them has been shown to be universally valid. We use the model by *Winterwerp* [1998] as this comprises a small number of parameters and is expressed as a function of the floc size and fractal dimension. By substituting $d_3(L)$ into Winterwerp's model we obtain

$$B = E\left(\frac{\mu}{F_y}\right)^{1/2} G^{3/2} L \left(\frac{L}{L_{\mathrm{p}}} - 1\right)^{3-d_3(L)}, \tag{14}$$

where E is a breakup parameter in the order 10^{-6} m^{-1}, $F_y = 10^{-10}$ Pa is an estimate floc strength, and $d_3(L)$ is as in equation (4). Model results in Figure 9 show that the frequency of breakup, low for small flocs, increases more rapidly from floc sizes $L \simeq 40$ μm because of a d_3 decreasing with L compared to B computed with constant

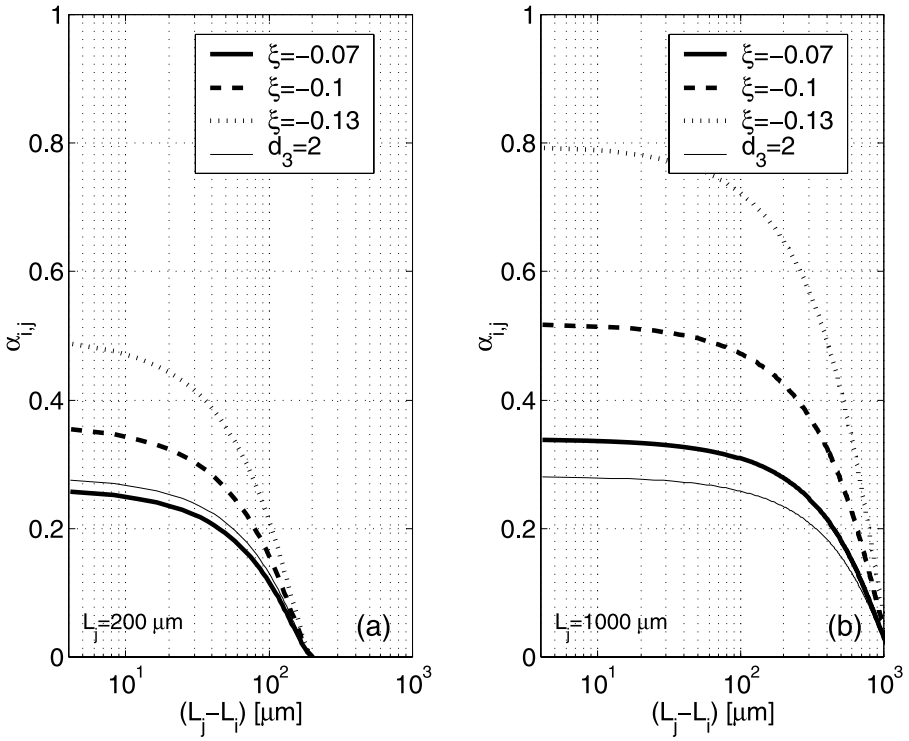

Figure 8. Collision efficiency computed for (a) the range of floc sizes $L_i = 4–200$ μm with a floc of size $L_j = 200$ and for (b) the range of floc sizes $L_i = 4–1000$ μm with a floc of size $L_j = 1000$ for constant and variable capacity dimensions d_3, the latter computed for $\delta = 3$ and various values of ξ. Differences from using equation (4) and $d_3 = 2$ can be larger than a factor 2.

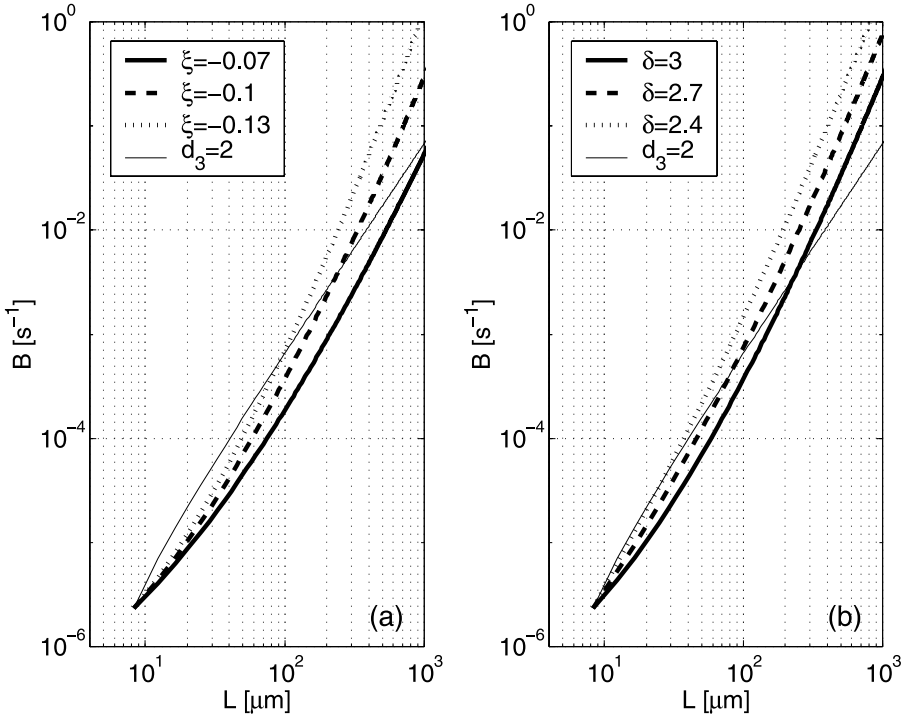

Figure 9. Breakup frequency as a function of L for constant and variable capacity dimensions d_3, the latter computed for various values of (a) ξ and (b) δ. Difference from using equation (4) and $d_3 = 2$ can be of approximately 1 order of magnitude.

capacity dimension. Decreasing values of ξ and δ accentuate further this behavior.

5. Conclusions

[34] Experimentally acquired data has shown that the fractal dimension of suspended flocs changes within a floc size ranging more than 2 orders of magnitude. A power law function has been proposed to describe these changes. Analysis of this description of floc structure has shown that floc porosity, excess density, and settling velocity, as well as the kinematics of aggregation and breakup, can change from a factor of 2 up to 1 order of magnitude or more with respect to models with constant fractal dimension. Hence a variable fractal dimension is a major control for floc structure and flocculation kinematics of suspended cohesive sediment. This can in turn exert a substantial effect on larger time and length scales of flocculation and, consequently, of geophysical flows such as sediment transport and deposition in aqueous environments.

[35] In general terms, a wider experimental and mathematical effort can shed further light to these aspects. However, it is part of the author's plan to make a specific step forward into this direction by implementing this model for variable fractal dimension in a population balance equation based on Smoluchowski's equation [e.g., *Serra and Casamitjana*, 1998c; *Lick and Lick*, 1988; *Flesch et al.*, 1999] and assess its validity with the support of existing data.

[36] **Acknowledgments.** The author is grateful to Jurjen Battjes, Han Winterwerp, Gabriel Katul, and Amilcare Porporato for their constructive suggestions and to the BEO-Programme from the TUDelft Research Funds for financing the experimental activity. The author would like to thank also the two anonymous reviewers for their encouraging comments and fruitful suggestions to this work.

References

Argyris, J., G. Faust, and M. Haase (1994), *An Exploration of Chaos*, John Argyris F.R.S, North-Holland, Amsterdam.

Ball, R., and M. Blunt (1989), Screening in multifractal growth, *Phys. Rev. A*, *39*(7), 3591–3596.

Berka, M., and J. A. Rice (2005), Relation between aggregation kinetics and the structure of kaolinite aggregates, *Langmuir*, *21*, 1223–1229.

Burban, P. Y., W. Lick, and J. Lick (1989), The flocculation of fine-grained sediments in estuarine waters, *J. Geophys. Res.*, *94*(4), 514–523.

Burd, A., and G. A. Jackson (1997), Predicting particle coagulation and sedimentation rates for a pulsed input, *J. Geophys. Res.*, *102*(C5), 10,545–10,561.

Chakraborti, R. K., K. H. Gardner, J. F. Atkinson, and J. E. van Benschoten (2003), Changes in fractal dimension during aggregation, *Water Res.*, *37*, 873–883.

Chhabra, A., and R. V. Jensen (1989), Direct determination of the f(α) singularity spectrum, *Phys. Rev. Lett.*, *62*(12), 1327–1330.

Falconer, K. (1990), *Fractal Geometry; Mathematical Foundations and Applications*, Wiler, Chichester.

Farley, K. J., and F. M. M. Morel (1986), Role of coagulation in the kinetics of sedimentation, *Environ. Sci. Technol.*, *20*, 187–195.

Flesch, J. C., P. T. Spicer, and S. E. Pratsinis (1999), Laminar and turbulent shear-induced flocculation of fractal aggregates, *AIChE J.*, *45*(5), 1114–1124.

Friedlander, S. K. (1957), Mass and heat transfer to single spheres and cylinders at low Reynolds number, *AIChE J.*, *3*, 43–48.

Friedlander, S. K. (1965), The similarity theory of the particle size distribution of the atmospheric aerosols, in *Aerosols, physical chemistry and application*, edited by K. Spurny, p. 115–130, Czechoslovakian Academy of Science, Prague.

Gardner, K. H., T. L. Theis, and T. C. Young (1998), Colloid aggregation: Numerical solution and measurements, *Colloids Surf., A*, *141*, 237–252.

Grassberger, P., and I. Procaccia (1983), Characterization of strange attractors, *Phys. Rev. Lett.*, *50*(5), 346–349.

Hentschel, H. G. E., and I. Procaccia (1983), The infinite number of generalized dimensions of fractals and strange attractors, *Physica*, *8*(D), 435–444.

Hunt, J. R. (1980), Prediction of oceanic particle size distribution from coagulation and sedimentation mechanisms, *Advances in Chemistry* vol. 189, Particle in Water, edited by M. D. Kavanaugh and J. T. Kekie, pp. 243–257, American Chemical Society.

Johnson, C. P., X. Li, and B. E. Logan (1996), Settling velocities of fractal aggregates, *Environ. Sci. Technol.*, *30*, 1911–1918.

Jullien, R., and P. Meakin (1989), Simple models for the restructuring of three-dimensional ballistic aggregation, *J. Colloid Interface Sci.*, *127*, 265–272.

Khelifa, A., and P. S. Hill (2006), Models for effective density and settling velocity of flocs, *J. Hydraul. Res.*, *44*, 390–401.

Kim, A. S., and K. D. Stolzenbach (2004), Aggregate formation and collision efficciency in differential settling, *J. Colloid Interface Sci.*, *271*, 110–119.

Kim, A. S., and R. Yuan (2005), Hyrodynamics of an ideal aggregate with quadratically increasing permeability, *J. Colloid Interface Sci.*, *285*, 627–633.

Kranenburg, C. (1994), the fractal structure of cohesive sediment aggregates, *Cont. Shelf Sci.*, *39*, 451–460.

Krishnappan, B. C. (1990), Modelling of settling and flocculation of fine sediments in still water, *Can. J. Civil Eng.*, *17*, 763–770.

Kunster, K. A., J. G. Wijers, and D. Thoenes (1997), Aggregation kinetics of small particles in agitated vessels, *Chem. Eng. Sci.*, *52*(1), 107–121.

Li, X.-Y., and B. E. Logan (1997), Collision Frequencies between fractal aggregates and small particles in a turbulently sheared fluid, *Environ. Sci. Technol*, *31*, 1237–1242.

Li, X.-Y., and B. E. Logan (2001), Permeability of fractal aggregates, *Water Res.*, *35*(14), 3373–3380.

Lick, W., and J. Lick (1988), On the aggregation and disaggregation of fine-grained sediments, *J. Great Lakes Res.*, *14*(4), 514–523.

Lick, W., H. Huang, and R. Jepsen (1993), Flocculation of Fine-Grained Sediments due to Differential Settling, *J. Geophys. Res.*, *98*((C6)-10), 279–288.

Maggi, F. (2005), Flocculation dynamics of cohesive sediments, Ph.D. thesis, Delft Universitiy of Technology, Netherlands.

Maggi, F., and J. C. Winterwerp (2004), Method for computing the three-dimensional capacity dimension from two-dimensional projections of fractal aggregates, *Phys. Rev. E*, *69*, 011405.

Maggi, F., J. C. Winterwerp, H. L. Fontijn, W. G. M. van Kesteren, and J. M. Cornelisse (2002), A settling column for turbulence-induced flocculation of cohesive sediments, *Proceedings of HMEM2002 Conference*, edited by T. L. Wahl, C. A. Pugh, K. A. Oberg, and T. B. Vermeyen, Estes Park, Colorado, paper 93, doi:10.1061/40655(2002)34.

Maggi, F., A. J. Manning, and J. C. Winterwerp (2006), Image separation and geometric characterisation of mud flocs, *J. Hydrol.*, *326*, 325–348.

Manning, A. J., and K. R. Dyer (1999), A laboratory examination of floc characteristics with regard to turbulent shearing, *Mar. Geol.*, *160*, 147–170.

Manning, A. J., and K. R. Dyer (2002), The use of optics for the in situ determination of flocculated mud characteristics, *J. Opt. A*, *4*, S71–S81.

McCave, I. N. (1984), Size spectra and aggregation of suspended particles in the deep ocean, *Deep-Sea Res.*, *31*(4), 329–352.

Meakin, P. (1991), Fractals aggregates in geophysics, *Rev. Geophys.*, *29*.

Meakin, P. (1998), *Fractals, Scaling and Growth Far From Equilibrium*, Cambridge Univ. Press, Cambridge.

Neimark, A. V., Ü. O. Köylü, and D. E. Rosner (1996), Extended characterization of combustion-generated aggregates: Self-affinity and lacunarities, *J. Colloid Interface Sci.*, *180*, 590–597.

Oles, V. (1992), Shear-induced aggregation and breakup of polystyrene latex particles, *J. Colloid Interface Sci.*, *154*, 351–358.

Pruppacher, H. R., and J. D. Klett (1978), *The Microphysics of Clouds and Precipitation*, Springer, New York.

Sato, D., M. Kobayashi, and Y. Adachi (2004), Effect of floc structure on the rate of shear coagulation, *J. Colloid Interface Sci.*, *272*, 345–351.

Serra, T., and X. Casamitjana (1998a), Effect of the shear volume fracton on the aggregation and break-up of particle, *American Institute of Chemical Engineers*, *44*(8), 1724–1730.

Serra, T., and X. Casamitjana (1998b), Structure of the aggregates during the process of aggregation and break-up under a shear flow, *J. Colloid Interface Sci.*, *206*, 505–511.

Serra, T., and X. Casamitjana (1998c), Modelling the aggregation and break-up of fractal aggregates in shear flow, *Appl. Sci. Res.*, *59*, 255–268.

Spicer, P. T., S. E. Pratsinis, J. Raper, R. Amal, G. Bushell, and G. Meesters (1998), Effect of shear schedule on particle size, density, and structure during flocculation in stirred tanks, *Powder Technol.*, *97*, 26–34.

Sterling, M. C., J. S. Bonner, A. N. S. Ernest, C. A. Page, and R. L. Autenrieth (2005), Aplication of fractal flocculation and vertical transport model to aquatic sol-sediment systems, *Water Res.*, *39*, 1818–1830.

Stolzenbach, K. D., and M. Elimelech (1993), The effect of particle density on collision between sinking particles: implications for Particle aggregation in the ocean, *Deep-Sea Res., Part I*, *41*(3), 469–483.

Stone, M., and B. G. Krishnappan (2003), Floc morphology and size distributions of chesive sediment in steady flow, *Water Res.*, *37*, 2739–2747.

Thill, A., S. Moustier, J. Aziz, M. R. Wiesner, and J. Y. Bottero (2001), Floc restructuring during aggregation: Experimental evidence and numerical simulation, *J. Colloid Interface Sci.*, *243*, 171–182.

Van Leussen, W. (1994), Estuarine Macroflocs, Ph.D. thesis, University of Utrecht, Netherlands.

Veerapaneni, S., and M. R. Wiesner (1996), Hydrodynamics of fractal aggregates with radially varying permeability, *J. Colloid Interface Sci.*, *177*, 45–57.

Vicsek, T. (1992), *Fractal Growth Phenomena*, World Sci., Hackensack, N. J.

Winterwerp, J. C. (1998), A simple model for turbulence induced flocculation of cohesive sediment, *J. Hydraul. Eng. Res.*, *36*(3), 309–326.

Wu, R. M., D. L. Lee, T. D. Waite, and J. Guan (2002), Multilevel structure of sludge flocs, *J. Colloid Interface Sci.*, *252*, 383–392.

Zhang, J.-J., and X.-Y. Li (2003), Modeling Particle-Size Distribution Dynamics in a Flocculation System, *AIChE J.*, *49*(7), 1870–1882.

F. Maggi, Civil and Environmental Engineering, 760 Davis Hall, University of California, Berkeley, CA 94720-1710, USA. (fmaggi@berkeley.edu)